Clutter Mitigation using Auxiliary Elements for the NWRT Phased Array Radar

K. D. Le [†*1], R. D. Palmer [†#], B. L. Cheong [†#], T. Y. Yu [†*], G. Zhang [†#], and S. M. Torres [†°]

[†]*Atmospheric Radar Research Center*
Norman, OK 73072, USA
[1]khoi@ou.edu

[*]*Department of Computer and Electrical Engineering, University of Oklahoma*

[#]*School of Meteorology, University of Oklahoma*

[°]*NOAA/OAR National Severe Storms Laboratory*
Norman, OK 73072, USA

[°]*Cooperative Institute of Mesoscale Meteorological Studies (CIMMS)*
Norman, OK 73072, USA

***Abstract*— The National Weather Radar Testbed (NWRT) has a 10-cm phased array radar that is used primarily for monitoring the weather. It is attractive compared to the current parabolic dish Weather Surveillance Radar-88 Doppler (WSR-88D) because of its capability to electronically steer. When combined with the recently developed beam multiplexing technique that uses a small number of contiguous samples and clever spatial sampling, this radar can obtain very rapid update scans and is extremely advantageous in monitoring severe weather. However, the small number of contiguous samples makes filtering of the clutter signal problematic in the temporal/spectral domain and can limit the performance of this radar in clutter dominated conditions. By exploiting the spatial correlation of the auxiliary channel signals, the effect of clutter contamination can be reduced to overcome this problem. In this work, two spatial filtering techniques that use low-gain auxiliary receive channels are presented, and the effect of clutter mitigation is investigated using numerical simulations for a tornadic thunderstorm dominated by clutter return. Parameters under investigation include signal-to-noise ratio, clutter-to-signal ratio, number of time series samples, varying clutter spectral widths, and maximum weight constraints.**

I. Introduction

The National Weather Radar Testbed, which is located in Norman, Oklahoma, has a 10-cm phased array radar that became operational in 2003 [1]. The radar consists of an Aegis SPY-1A antenna and a WSR-88D transmitter. It serves to test the operational utility of phased array radars (PAR) in monitoring the weather [1] and analyzing the evolution of severe storms to provide early warning. Examples of ongoing research at the testbed include beam-multiplexing [2], simultaneous aircraft tracking and weather surveillance [3], spaced-antenna interferometry (SAI) to measure crossbeam wind and to detect/locate sub-volume inhomogeneity [4], [5], monopulse processing [6], and the extraction of atmospheric refractivity from the scattering of ground targets [7]. Preliminary results of storm evolution [8] and microburst [9] comparisons between the PAR, WSR-88D, and Terminal Doppler Weather Radar are promising. The NWRT is quickly becoming an ideal resource for obtaining information on the effectiveness, advantage, and limitations of phased array radars under operational and research conditions for the surveillance of weather.

When combined with beam multiplexing (BMX), phased array radars such as the NWRT can obtain rapid update scanning strategies without compromising data accuracy. According to [2], BMX can reduce the acquisition time up to four times when the received Signal-to-Noise Ratio (SNR) is larger than 10 dB. Unfortunately, the number of contiguous time samples is small when using this scanning strategy as it involves resampling the scattering region over many revisits. This is problematic for conventional clutter filters since the number of contiguous samples is generally less than their impulse response. Because phased array radars consist of multiple received elements, the spatial correlation between the elements can be used to filter the clutter instead.

In this work, the focus is the applicability of spatial filtering and phased array for weather observations when the number of contiguous samples is small. Though spatial filtering may be applied to all the receive elements of the phased array, the examined techniques are limited to partially adaptive arrays, which the NWRT PAR would become after its next major upgrade.

II. Partially Adaptive Arrays

The next major hardware upgrade of the NWRT PAR is to add several auxiliary elements to the main array An example of such a configuration is illustrated in Figure 1. This array configuration was first introduced by [11].

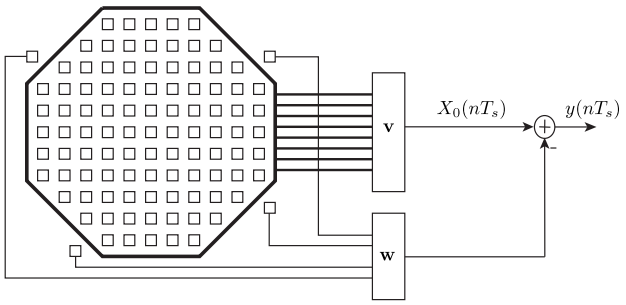

Fig. 1. Depiction of a partially adaptive array. The signal in the upper path is obtained by forming a nonadaptive radiation pattern in the steered direction with weights $\mathbf{v}$, and the lower channel is obtained using adaptive weights $\mathbf{w}$, which is selected by some optimization scheme. The output signal is obtained by subtracting the adaptive signal from the nonadaptive signal.

Accordingly, the output signal of the partially adaptive array is defined as

$$y(nT_s) \quad = \quad X_0(nT_s) - \mathbf{w}^H \mathbf{x}(nT_s), \tag{1}$$

where the output time series of the main channel is $X_0(nT_s)$, the vector of time series of the auxiliary channel is $\mathbf{x}(nT_s)$, and the weight vector of the auxiliary channel is $\mathbf{w}$. The time series and weight vectors are both column vectors and the length of each vector is equal to the number of auxiliary channels. The Hermitian operator is $(\cdot)^H$ and the sampling time is T_s.

Additionally, the correlation matrix at zero temporal lag of the auxiliary signals is

$$\mathbf{R} \quad = \quad \mathrm{E}\{\mathbf{x}(nT_s)\mathbf{x}^H(nT_s)\}. \tag{2}$$

The cross correlation vector between the main and auxiliary signals is $\mathbf{p} = \mathrm{E}\{\mathbf{x}(nT_s)X_0^*(nT_s)\}$.

1) Minimum Variance Distortionless Response: The Minimum Variance Distortionless Response (MVDR) of [18] is a technique used to obtain the optimal filter weights that satisfy a unity gain constraint in the steered direction and produce an output signal with the minimum averaged power [14]. The weights are obtained by defining the averaged output power as

$$\mathrm{E}\{y(nT_s)y^*(nT_s)\} \quad = \quad \mathrm{E}\{|X_0(nT_s) - \mathbf{w}^H \mathbf{x}(nT_s)|^2\}. \tag{3}$$

It follows that the minimization problem is

$$\min_{\mathbf{w}} \mathrm{E}\{|X_0(nT_s) - \mathbf{w}^H \mathbf{x}(nT_s)|^2\} \quad \text{subject to} \quad \mathbf{w}^H \mathbf{e} = 0, \tag{4}$$

where the steering vector is $\mathbf{e}$, which simply is the array response in that directionBased on the constraint, it is desired that the output signal in the steered direction is left unaltered. Since $X_o(t)$ is not weighted, it is easier to solve the problem by defining

$$\tilde{\mathbf{w}} \quad = \quad \begin{bmatrix} w_0 \\ -\mathbf{w} \end{bmatrix}, \tag{5}$$

and

$$\tilde{\mathbf{R}} \quad = \quad \mathrm{E}\left\{ \begin{bmatrix} X_0(nT_s) \\ \mathbf{x}(nT_s) \end{bmatrix} \begin{bmatrix} X_0(nT_s) \\ \mathbf{x}(nT_s) \end{bmatrix}^H \right\}. \tag{6}$$

The averaged output power is then

$$\begin{aligned} \mathrm{E}\{y(nT_s)y^*(nT_s)\} \quad &= \quad \mathrm{E}\left\{ \left| \begin{bmatrix} w_0 \\ -\mathbf{w} \end{bmatrix}^H \begin{bmatrix} X_0(nT_s) \\ \mathbf{x}(nT_s) \end{bmatrix} \right|^2 \right\} \\ &= \quad \tilde{\mathbf{w}}^H \tilde{\mathbf{R}} \tilde{\mathbf{w}}. \end{aligned} \tag{7}$$

Let

$$\tilde{\mathbf{E}} \quad = \quad \begin{bmatrix} 1 & 1 \\ -\mathbf{e} & \mathbf{0} \end{bmatrix}, \tag{8}$$

where $\mathbf{0}$ is a column vector of 0's with length equal to the number of auxiliary channels, and $\tilde{\mathbf{1}} = \begin{bmatrix} 1 & 1 \end{bmatrix}$. The constraint in the second column forces w_0 to be unity.

Using quadratic minimization to solve the problem

$$\min_{\tilde{\mathbf{w}}} \tilde{\mathbf{w}}^H \tilde{\mathbf{R}} \tilde{\mathbf{w}} \quad \text{subject to} \quad \tilde{\mathbf{w}}^H \tilde{\mathbf{E}} = \tilde{\mathbf{1}} \tag{9}$$

results in

$$\tilde{\mathbf{w}}_o \quad = \quad \tilde{\mathbf{R}}^{-1} \tilde{\mathbf{E}} \left(\tilde{\mathbf{E}}^H \tilde{\mathbf{R}}^{-1} \tilde{\mathbf{E}} \right)^{-1} \tilde{\mathbf{1}}^H. \tag{10}$$

2) Subspace Tracking Spatial Projection: The Subspace Tracking Spatial Projection (STSP) of [19], designed to mitigate radio frequency interference of phased array radio telescopes, is a technique used to obtain the optimal weights constrained to be in the subspace of the clutter and produces an output signal that is not composed of any clutter component. The optimal weights of the STSP are obtained by projecting the weights of the multiple sidelobe canceller ([17]) onto the clutter subspace, defined by the correlation matrix $\mathbf{R}_i$.

The minimization problem is stated as the following

$$\min_{\mathbf{w}} \mathrm{E}\{y(nT_s)y^*(nT_s)\} \quad \text{subject to} \quad \mathbf{w}_o \in \mathbf{R}_i. \tag{11}$$

In the minimization problem, $\mathbf{w}_o \in \mathbf{R}_i$ implies that the output weights is a subspace of the clutter space. In [19], STSP was formulated to reduce the mainlobe distortion and high sidelobe levels produced by the optimal weights obtained from the MVDR technique. In this work, the methodology is applied to the optimal weights obtained from the MSC. Thus,

$$\mathbf{w}_o \quad = \quad \mathbf{P}_i^{\parallel} \mathbf{R}^{-1} \mathbf{p}, \tag{12}$$

where $\mathbf{P}_i^{\parallel} = \mathbf{U}_i \mathbf{U}_i^{\dagger}$, with $\mathbf{U}_i^{\dagger} = (\mathbf{U}_i^H \mathbf{U}_i)^{-1} \mathbf{U}_i^H$ and $\mathbf{U}_i$ are the clutter eigenvectors.

III. Numerical Simulations

Since the hardware upgrade has not been implemented and is several years away from completion, the performance of the clutter filtering techniques is investigated via numerical simulations. Evaluation of their performance in terms of bias and variance of the retrieved compared to the uncontaminated power will be investigated for variation in ϵ, CSR, SNR, NPTS, and standard deviation of clutter spectral widths, σ_c.

A. Radar Configuration and Environmental Fields

The simulator of [20] was used in generating the time series signals. An illustration depicting the simulator is plotted in Figure 2. This simulator uses point targets to model the environmental and clutter field. The point targets that emulate the weather field have scattering and dynamic properties obtained from the Advanced Regional Prediction System (ARPS) [21], [22].

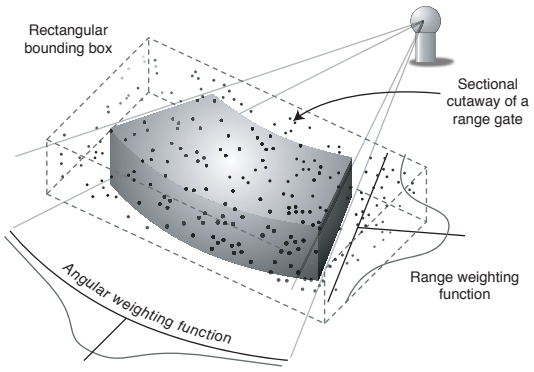

Fig. 2. Depiction of simulator. Point source scatterers with reflectivity and dynamic properties derived from the ARPS model are used to emulate the scattering field. In contrast, their reflectivity is constant and the motion is random for those that emulate the clutter field.

The weather field simulated is a tornadic event initiated using the 20 May 1977 Del City, Oklahoma upper air sounding [23]. Parameters used in the simulation are listed in Table I. Fifty thousand point targets were used to model the environmental field and 1,000 point targets were used to model the clutter field. These targets occupied a volume of approximately 7x7x5 km^3 with the radar located approximately 33 km from this volume. The positions of the elements of the radar are drawn in Figure 3. The main receiver is composed of 4352 elements, and the sidelobe canceler is composed of six auxiliary elements situated around the main receiver. The aperture of the combined radar is approximately 3.6x3.8 m^2, and its receive beamwidth is approximately 1.6° at broadside while its transmit beamwidth was selected to be 20°. The range resolution was 235 m while the aliasing velocity was 23.4 m s^{-1} using a PRF of 10^3 Hz at $\lambda = 0.1$ m. The radar observed the simulated tornadic event over a 200 s duration at 25 s interval, 256 time series samples were collected during each scan.

TABLE I
SIMULATION PARAMETERS

Simulated volume (Zonal x Meridional x AGL)	$7 \times 7 \times 5$ km^3
Number of atmospheric scatterers	50,000
characteristics	ARPS-derived
Number of ground clutter scatterers	1,000
characteristics	constant reflectivity random motion
Transmit antenna beamwidth	20°
Receive aperture (width x height)	3.6×3.8 m^2
Number of main array elements	4352
Number of auxiliary elements	6
Pulse repetition frequency	1000 Hz
Frequency	3 GHz
Aliasing velocity	23.4 m s^{-1}
Number of pulses	256
Range resolution	235 m

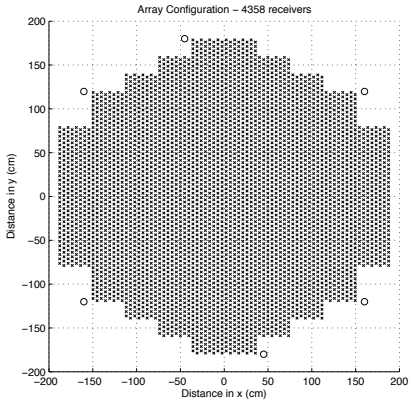

Fig. 3. Positions of receiving elements. The array consists of 4352 elements (×) that make up the main channel and six auxiliary elements (○). The aperture of the array is approximately 3.6 m × 3.8 m (width×height), producing a beamwidth of ≈1.6° at broadside.

IV. PRELIMINARY RESULTS

The performance of the SLC techniques appears to be strongly controlled by the diagonal loading value. An example showing this effect is plotted in Figure 4, which contains the results obtained using MVDR at t = 100 s and 3.5° for three amount of diagonal weights. The simulation parameters are CSR = 30 dB, SNR = 70 dB, σ_c = 0.1 m s^{-1}, and NPTS = 4. When the diagonal value is insufficient, clutter and weather signals are removed and a negative bias in the power is observed. In contrast, insufficient clutter suppression is observed when the diagonal value is too large and the field is saturated with the clutter signature.

Another factor that affects the performance of the SLC techniques is the clutter space used in STSP. Since this factor is not known *a priori*, it is obtained by assuming that the dominant signature return at the radar belongs to the clutter and consequently the eigenvector of the largest eigenvalue of $\mathbf{R}$ is that of the clutter. The results showing this effect are presented Figure 5. The simulation parameters are ϵ = 0.1, CSR = 30 dB, SNR = 70 dB, σ_c = 0.1 m s^{-1}, and NPTS = 4. The results obtained using the largest eigen subspace (eig-1) appear to be most like that of the weather. This implies that most of the clutter signal is subtracted out when the largest eigen subspace is used. In contrast, the results obtained using the second largest eigen subspace consists of clutter-like characteristics and imply that clutter is not being removed.

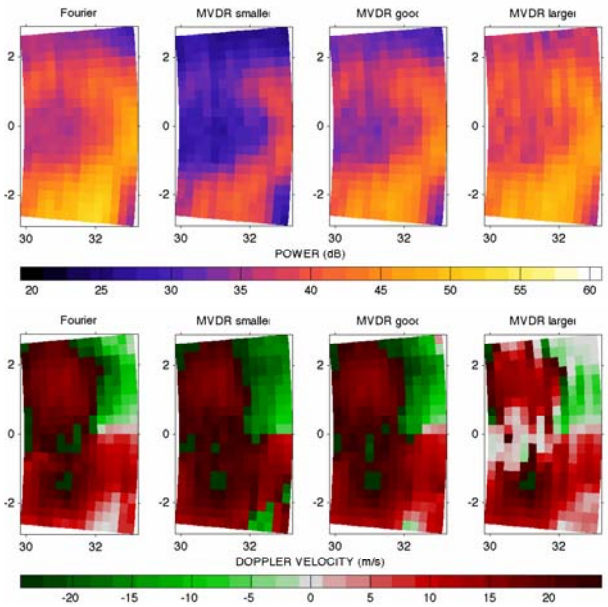

Fig. 4. Example of diagonal loading effect. Simulation parameters are CSR = 30 dB, SNR = 70 dB, σ_c = 0.1 m s^{-1}, and NPTS = 4. The fields were obtained at t = 100 s at 3.5°.

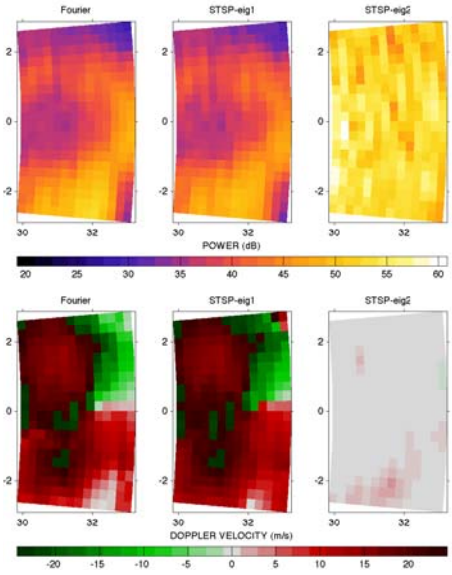

Fig. 5. Example of subspace selection effect. Simulation parameters are ϵ = 0.1, CSR = 30 dB, SNR = 70 dB, σ_c = 0.1 m s^{-1}, and NPTS = 4. The fields were obtained at t = 100 s at 3.5°.

ACKNOWLEDGMENT

This work is partially supported by the National Severe Storms Laboratory (NOAA/NSSL) under cooperative agreement NA17RJ1227.

REFERENCES

[1] D. Forsyth, J. Kimpel, D. Zrnic, S. Sandgathe, R. Ferek, J. Heimmer, T. M. J. Crain, J. Belville, and W. Benner, "Update on The National Weather Radar Testbed (Phased-Array)," in *23rd Conference on IIPS*, 14-18 January, San Antonio, TX, 2007.

[2] T.-Y. Yu, M. Orescanin, C. Curtis, D. Zrnic, and D. Forsyth, "Beam Multiplexing Using the Phased-Array Weather Radar," *J. Atmos. Oceanic Technol.*, vol. 24, no. 4, pp. 616–626, 2007.

[3] M. Yeary, B. McGuire, Y. Zhai, D. Forsyth, W. Benner, and G. Torok, "Target Tracking at The National Weather Radar Testbed: A Progress Report on Detecting and Tracking Aircraft," in *23rd Conference on IIPS*, 14-18 January, San Antonio, TX, 2007.

[4] G. Zhang, R. Doviak, and X. Chen, "Spaced-Antenna Interferometry to Detect Discrete Objects and Sub-Volume Inhomogeneities of Reflectivity," in *33rd Conference on Radar Meteorology*, 6-10 August, Cairns, Australia, 2007.

[5] G. Zhang and R. Doviak, "Interferometry to Measure Crossbeam Wind, Shear, and Turbulence: Theory and Formulation," *J. Atmos. Oceanic Technol.*, vol. 24, no. 5, pp. 791–805, 2007.

[6] M. Teshiba, T. Yu, G. Crain, and M. Xue, "A Monopulse System: Applications for Weather Radar Observations," in *33rd Conference on Radar Meteorology*, 6-10 August, Cairns, Australia, 2007.

[7] B. Cheong, R. Palmer, C. Curtis, T.-Y. Yu, D. Zrnic, and D. Forsyth, "Refractivity Measurements From Ground Clutter Using the Nation Weather Radar Testbed Phased Array Radar," in *23rd Conference on IIPS*, 14-18 January, San Antonio, TX, 2007.

[8] P. Heinselman, D. Priegnitz, K. Manross, and R. Adams, "Comparison of Storm Evolution Characteristics: The NWRT and WSR-88D," in *33rd Conference on Radar Meteorology*, 6-10 August, Cairns, Australia, 2007.

[9] T. Smith, P. Heinselman, and D. Priegnitz, "Characteristics of Microburst Events Observed with the National Weather Radar Testbed Phased Array Radar," in *23rd Conference on IIPS*, 14-18 January, San Antonio, TX, 2007.

[10] B. Cheong, M. Hoffman, R. Palmer, S. Frasier, and F. Lopez-Dekker, "Phased-Array Design for Biological Clutter Rejection: Simulation and Experimental Validation," *J. Atmos. Oceanic Technol.*, vol. 23, no. 4, pp. 585–598, 2006.

[11] P. Howells, "Intermediate Frequency Sidelobe Cancellers," Patent, 1965, u.S. Patent 3202990.

[12] D. Manolakis, V. Ingle, and S. Kogon, *Statistical and Adaptive Signal Processing: Spectral Estimation, Signal Modeling, Adaptive Filtering and Array Processing*. Boston: McGraw Hill, 2000.

[13] B. Farhang-Boroujeny, *Adaptive Filters: Theory and Application*. New York: John Wiley & Sons, 1998.

[14] S. Haykin, *Adaptive Filter Theory: Third Edition*. New Jersey: Prentice Hall, 1996.

[15] R. Monzingo, T. Miller, and W. Thomas, *Introduction to Adaptive Arrays*. Raleigh, NC: SciTech Publishing, 2004.

[16] B. Carlson, "Covariance Matrix Estimation Errors and Diagonal Loading in Adaptive Array," *IEEE Trans. Aerosp. Electron. Syst.*, vol. 24, no. 4, pp. 397–401, 1988.

[17] B. Widrow, P. Mantey, L. Griffiths, and B. Goode, "Adaptive Antenna Systems," *Proc. IEEE*, vol. 55, no. 12, pp. 2143–2159, 1967.

[18] J. Capon, "High-Resolution Frequency-Wavenumber Spectrum Analysis," *Proc. IEEE*, vol. 57, no. 8, pp. 1408–1418, 1969.

[19] S. Ellingson and G. Hampson, "A Subspace-Tracking Approach to Interference Nulling for Phased Array-Based Radio Telescope," *IEEE Trans. Anten. Prop.*, vol. 50, no. 1, pp. 25–30, 2002.

[20] B. Cheong, R. Palmer, and M. Xue, "A Time-Series Weather Radar Simulator Based on High-Resolution Atmospheric Models," *J. Atmos. Oceanic Technol.*, 2007, accepted.

[21] M. Xue, K. Droegemeier, and V. Wong, "The Advanced Regional Prediction System (ARPS) - A multi-scale nonhydrostatic atmospheric simulation and prediction model. Part I: Model dynamics and verification," *Meteor. Atmos. Physics.*, vol. 75, no. 3-4, pp. 161–193, 2000.

[22] M. Xue, K. Droegemeier, V. W. A. Shapiro, K. Brewster, F. Carr, D. Weber, Y. Liu, and D. Wang, "The Advanced Regional Prediction System (ARPS) - A multi-scale nonhydrostatic atmospheric simulation and prediction model. Part II: Model physics and applications," *Meteor. Atmos. Physics.*, vol. 76, no. 3-4, pp. 143–165, 2001.

[23] P. Ray, B. Johnson, K. Johnson, J. Bradberry, J. Stephens, K. Wagner, R. Wilhelmson, and J. Klemp, "The Morphology of Several Tornadic Storms on 20 May 1977," *J. Atmos. Sci.*, vol. 38, no. 8, pp. 1643–1663, 1981.